

# POLARIZATION INFLUENCE ON THE EFFICIENCY, THE SIGNAL AND THE NOISE OF BLEACHED SILVER HALIDE DIFFUSE-OBJECT HOLOGRAMS

---

A. Fimia, R. Fuentes, I. Pascual, and A. Beléndez<sup>(†)</sup>

Laboratorio de Optica. Departamento Interuniversitario de Optica  
Universidad de Alicante. Apdo. nº 99. E-03080 Alicante. SPAIN

(†) Departamento de Ingeniería de Sistemas y Comunicaciones  
Universidad de Alicante. Apdo. nº 99. E-03080 Alicante. SPAIN  
*Member of SPIE*

Phone: + 34 - 6 - 590 35 09

Fax: + 34 - 6 - 590 34 64

e-mail: [fimia@vm.cpd.ua.es](mailto:fimia@vm.cpd.ua.es)

---

*This paper is a revision of Paper 2406-12 which was presented at the IS&T/SPIE symposium in Electronic Imagieng, Science and Technology (Practical Holography IX), February 5-10, 1995, San José, California. The paper presented here appears (unrefereed) in SPIE proceedings Vol. 2406.*

## ABSTRACT

The efficiency and the noise of diffuse-object holograms recorded as volume holograms in bleached silver halide emulsion are experimentally analyzed as a function of the polarization state of the readout wave. An important source of noise found in these holograms when they are processed with rehalogenating bleaches are noise gratings which are very sensitive to polarization. The dependence of signal-to-noise ratio on the relative polarization between the construction and reconstruction beam is shown too. Experimental results are presented which make it possible to choose the best reconstruction conditions for these holograms.

**Keywords:** Holographic recording materials, silver halide emulsions, noise gratings, polarization.

## 1. INTRODUCTION

Nowadays, Holography is increasingly important in different fields of Optical Technology and many types of holograms are now being used for scientific and technical applications. For example, holograms are among the most important components for optical computing. In several important applications of holography such as optical interconnects or optical information storage it is necessary to multiplex several functions or many optical components in the same thin film recording material. An optically recorded multiple grating hologram can be encoded either sequentially or simultaneously, but for the same total exposure, the diffraction efficiency of sequentially recorded holograms is lower than for a simultaneous hologram. If the number of multiplexed gratings is increased, and the angles between these gratings are reduced, the recorded object beam should resemble the field from a diffuse-object<sup>1</sup>. On the other hand, the theoretical maximum storage density (bit per unit of hologram area) of an ideal (noise-free) thick hologram is proportional to the hologram thickness<sup>2</sup>. However, in actual holograms, noise is present and it seriously limits that density. That is why maximum storage density is a function of the hologram's signal-to-noise ratio (SNR). For all of these reasons it is important to analyze the characteristics of diffuse-object holograms in the field of optical interconnects<sup>3</sup> or information storage<sup>4,5</sup>.

An ideal holographic recording reconstructs a wavefront whose complex amplitude is linearly proportional to that of the original signal wavefront. Properties of the recording which cause light other than that proportional to the signal, to diffract into the direction of the signal wave may be regarded as sources of noise. Dielectric holograms typically reconstruct a brighter image than absorption holograms, but these holograms have greatly reduced contrast, or a higher noise level. This decrease in quality is caused by a number of factors, some of which are inherent in the characteristics of dielectric recording and some of which are caused by imperfections in the recording material. We can presumably improve the recording materials, but we cannot entirely eliminate the noise

inherent in the dielectric recording process. This can be reduced by the proper choice of recording parameters and chemical processing.

Volume phase holograms are attractive for use as optical elements or for holographic storage due to their high potential efficiency and high information densities. However no ideal holographic recording material has yet been found. One of the most common materials is photographic emulsion. Bleached silver halide emulsions are worthy of being considered as a volume holographic material because of several attractive advantages that they offer. These advantages include a relatively high sensitivity and ease of processing, improved processing chemistries and high efficiency. This is also an ideal material for the experimental testing of holographic concepts, theoretical models such as Kogelnik's<sup>6</sup> or the EHGM<sup>7</sup>, for example, or for the analysis of many noise sources that are present in Holography<sup>8</sup>. Also, volume phase holograms recorded in photographic emulsions are of great interest owing to their use as holographic optical interconnects or holographic optical memories. Unfortunately, while the resulting phase holograms have high diffraction efficiency, this is usually accompanied by an increase in the scattering of light from the silver halide grains<sup>9</sup> and a consequent reduction in image quality. Scattering is due to the granular structure of the silver halide material and takes place both at the recording and at the reconstruction stage. During formation of a hologram, object fields scattered by the silver halide grains of the photographic emulsions interfere with the unscattered portion of the illuminating beam (which works as a reference beam), and because of this, spurious gratings are recorded in the medium<sup>10</sup>. During the reconstruction stage of the hologram, these self-induced gratings (called noise gratings) diffract light in directions other than that of the signal beam, and this gives rise to a reduction in the diffraction efficiency and in the quality of the intentionally formed hologram. The efficiency of these noise gratings depends to a great extent on the chemical processing (if the process introduces very small emulsion thickness changes, the noise grating efficiency is quite pronounced), the relative polarization between the recording and reconstruction beams, exposure, the beam ratio and the reconstruction wavelength.

During the reconstruction step of the holograms there is also scattering of light from individual grains of the processed photosensitive medium in which the hologram is formed. This source of noise -"scattering"- becomes important when the diffraction efficiency is low. Low diffraction efficiency is unavoidable when the hologram plate must be exposed briefly to a weakly reflecting subject or when a larger number of absorption holograms are sequentially superimposed on the same plate<sup>11</sup>. However, in the experimental study that we developed, the object beam came from a transilluminated square glass diffuser and the plate was only exposed once. Moreover, we obtained phase holograms. Thus, this source of noise is not relevant.

Another important source of noise in dielectric diffuse-object holograms is intermodulation noise, which is a random-phase pattern that is caused by the self-interference of light from an extended object<sup>12-15</sup>. This phase structure is recorded as a variation of the refractive index within the emulsion and as a variation of the thickness of the layer because of the relatively low frequency of the pattern, however, the signal beam is recorded on a carrier that can be considered a volume recording, the intermodulation noise usually spans both the two dimensional and volume-recording, but basically it is two dimensional.

There is another type of noise that can be produced in phase holograms which is a result of the intrinsic nonlinearity of these holograms<sup>16</sup>. As an example of this, consider the simple case in which the final phase modulation,  $\phi(x)$ , to be imposed on the illuminating wave is simply proportional to exposure  $E(x)$ , say  $\phi(x) = \gamma E(x)$ , where  $\gamma$  is a proportionality constant between exposure and phase modulation (linear region of the H-D curve). The amplitude transmittance,  $t_a$ , defined as the ratio between the light amplitude transmitted and the light amplitude incident at the plate is given by:

$$t_a(x) = t_0 \exp [i \gamma E(x)] \quad (1)$$

where  $t_0$  is the average transmittance.

Most of the effect of this nonlinear relation between amplitude transmittance and exposure is to produce diffraction orders higher than first order diffractions. These orders are diffracted at angles that are two or more times the angle of the desired first-order image and thus are usually well separated from it. The existence of higher-order images is generally not important as long as they do not overlap the first-order images. The criterion for prevention of overlap is that the spatial bandwidth of the holographic signal modulating the carrier should be less than one-third the carrier frequency<sup>17</sup>. In our case this criterion was fulfilled as the incidence angle of the reference beam was  $37.5^\circ$  and the extreme points of the object formed a  $3.8^\circ$  angle from the central point of the plate. With this geometry the carrier frequency was  $\approx 1000$  lines/mm and the modulator frequency was  $\approx 100$  lines/mm, which is one-tenth of the carrier's. Therefore this noise source was eliminated, and the main sources of noise for the reconstructed image of the diffuse-object were noise gratings and intermodulation noise.

The polarization properties of thick hologram gratings are due to the different values of the coupling between the diffracted and incident waves inside the hologram for different directions of the electric vector of the incident wave, but these properties are more pronounced at high spatial frequencies than at low ones<sup>18</sup>. It is important to remember that intermodulation noise is a low-frequency noise and therefore it is not very sensitive to changes in the direction of the electric vector. This fact will be experimentally demonstrated in this paper.

Previous papers<sup>19,20</sup> have reported the influence of polarization on noise gratings but the studies have been done using a single collimated beam or two collimated beams. In another paper we showed<sup>21</sup> the presence of noise gratings in diffuse-object holograms as an important source of noise. The properties of diffuse-object holograms have been amply studied, but so far no detailed measurement of the influence of polarization has been reported, especially as regards the analysis of the influence of polarization on noise gratings in diffuse object holograms.

The aim of the present paper is to present experimental results on the influence of

the polarization angle (defined as the angle between the polarization vectors of the construction and reconstruction beams) on diffraction efficiency, noise and the signal-to-noise ratio of diffuse-objects holograms recorded in bleached silver halide emulsion.

## 2. FORMATION OF DIFFUSE-OBJECT HOLOGRAMS

Diffuse-object holograms were recorded on Agfa-Gevaert 8E75 HD emulsion and the exposures were made with 632.8 nm radiation from an He-Ne laser. The object used was a 2 cm x 2 cm square with a central opaque zone measuring 1 cm x 1 cm. The reference beam was collimated and it was polarized perpendicular to the plane of incidence. The distance of the object from the recording medium was 30 cm and the reference beam formed a 37.5° angle with the normal of the holographic plate which was parallel to the object. The reference-to-object beam ratio was  $K = 5$ .

Figure 1 shows a schematic representation of the geometry used in our experiments while in Figure 2 we show the diffuse-object used.

Twelve holograms were made with exposures ranging from 10 to 340  $\mu\text{J}/\text{cm}^2$ . Spurious reflections were eliminated by placement of an index-matched absorbing layer against the glass side of the photographic plate. After exposure, the plates were developed in PAAAC developer. The developed plates were rinsed briefly and bleached without a fixation step. Two types of bleach baths were used in these experiments: One was R-10 and the other was EDTA. Both of these are rehalogenating bleach baths. In these rehalogenating bleaches, the bleach baths contain a rehalogenating agent (potassium bromide) which converts most of the developed silver back into a silver halide. In this case a phase hologram is obtained mainly by the transfer of silver halide between the unexposed and exposed areas. These bleaches have the advantage that the resulting emulsion thickness change produced by these baths is very small ( $< 0.05 \mu\text{m}$ ) in the

nominally thick 6  $\mu\text{m}$  film<sup>22</sup>, since the overall removal of silver salts from the emulsion is minimal. Also it is assumed that the average refractive index does not change appreciably as a result of processing<sup>22</sup>. As thickness and the average refractive index of the holographic recording material show very little change when this type chemical processing is used, the reconstruction geometry of the holograms corresponding to maximum diffraction efficiency coincide with the construction geometry if recording and readout wavelengths are equal. This implies that Bragg's Law is complied with in the reconstruction stage, even though sometimes there is a displacement of the Bragg angle which is caused by shear-type effects<sup>23</sup>.

Details of the processing schedule as well as the developer and bleach bath formulas are given in Tables I and II.

### 3. MEASUREMENTS

The holograms were replayed in air with the conjugate of the collimated reference wave, and the diffracted output beam formed the real image of the object. The diffraction efficiency and the signal-to-noise ratio (SNR) were measured as a function of the replay angle using the same wavelength that was used during the recording stage. Measurements were obtained at 1-degree increments around the angle of the reference beam. The signal,  $S$ , was measured as the ratio between the average maximum light intensity of both sides of the square,  $I_1$  and  $I_2$ , of the reconstructed object and the incident light intensity,  $I_i$ , and the noise,  $N$ , was measured as the ratio between the minimum light intensity,  $I_o$ , in the central square of the reconstructed object and the incident light intensity,  $I_i$ :

$$S = \frac{I_1 + I_2}{I_i} \qquad N = \frac{I_o}{I_i} \qquad (2)$$



The following equation was used as SNR:

$$\text{SNR} = \frac{S}{N} = \frac{I_1 + I_2}{I_0} \quad (3)$$

Therefore the SNR give us the contrast at the reconstruted object. In all cases the experimental measurements for the intensities were corrected taking into account losses due to reflection at the two surfaces of the plates.

The plane defined by the emulsion surface normal and the electric field of the reference beam was used as a reference for the polarizations of both the recording and the replay beams. We define a polarization angle<sup>20</sup>,  $\delta$ , so that  $\delta = 0^\circ$  for the polarization of the reconstruction beam parallel to the polarization of the reference beam and  $\delta = 90^\circ$  when polarizations of the reference and reconstruction beams are perpendicular. In order to investigate the influence of polarization on diffraction efficiency, on the signal,  $S$ , and on the noise,  $N$ , of diffuse-object holograms, we measured these parameters for these two values of the polarization angle, i.e.,  $\delta = 0^\circ$  and  $\delta = 90^\circ$ .

#### 4. EXPERIMENTAL RESULTS AND DISCUSSION

In Figures 3 and 4 we can see the diffraction efficiency measurements as a function of the reconstruction angle for plates processed with EDTA and R-10 rehalogenating bleaches. In these figures the pronounced drop in diffraction efficiency at the reference angle ( $37.5^\circ$ ) when  $\delta = 0^\circ$  is caused by the presence of noise gratings. Furthermore we can see that the angular response of the diffraction efficiency is symmetrical around the recording angle for EDTA but not for R-10. In the latter case, there is a little displacement on the angular response which is not centered in the reference angle. As the thickness and the average refractive index of the emulsion did not change when a different type of processing was used, this displacement in the angular response

could be caused by shear-type effects<sup>7,23</sup>. When reconstruction is done with  $\delta = 90^\circ$  we see that the dip at the Bragg angle is eliminated and that the diffraction efficiency in this case is greater than with  $\delta = 0^\circ$ . However, this does not always occur but rather depends on both the exposure and the processing.

When we reconstructed the holograms with the Bragg angle ( $37.5^\circ$ ), the diffraction efficiency when  $\delta = 90^\circ$  was clearly greater than when  $\delta = 0^\circ$  for  $120 \mu\text{J}/\text{cm}^2$  for EDTA (Figure 5) and for  $30 \mu\text{J}/\text{cm}^2$  for R-10 (Figure 6).

Moreover it is also important to observe that if a different diffraction efficiency is obtained from this exposure for each polarization this is possibly due to having recorded an anisotropic periodic structure into the holographic emulsion.

Figures 7 and 8 show the results of the measurements of noise as a function of the reconstruction angle for plates processed with EDTA and R-10, respectively. As we can see, it is clear that when  $\delta = 90^\circ$ , the image has more noise than when  $\delta = 0^\circ$ . The measured noise with the two types of processing is similar when  $\delta = 0^\circ$ , but when  $\delta = 90^\circ$  noise is greater with R-10 than with EDTA. This might be due to the fact that when  $\delta = 90^\circ$ , the predominant source of noise is intermodulation noise which is a low-frequency noise and therefore very sensitive to emulsion thickness variations and consequently to the mechanism of material transfer. The R-10 diffusion coefficient<sup>24</sup> is greater than the EDTA coefficient and therefore amplifies the modulation of low-frequency better. This is why the peak noise for R-10 is greater than for EDTA.

Therefore, noise gratings are very sensitive to polarization; however as we said earlier, intermodulation noise is not very sensitive to changes in the direction of the electric vector. This can be experimentally confirmed when the processing used has a fixation step because in this case there are no noise gratings<sup>21</sup> and the main source of noise is intermodulation noise. Figure 9 shows these results.

Figures 10 and 11 show signal and noise as a function of the reconstruction angle for EDTA and R-10, respectively, when  $\delta = 0^\circ$ . As one can see from these figures, there is an interval of reconstruction angles (between  $38^\circ$  and  $41^\circ$ ) in which the signal

increases but not the noise. This uncoupling between the signal and the noise produces an increase in both the SNR and the diffraction efficiency, which is a very important fact. This does not occur when  $\delta = 90^\circ$ , as can be seen in Figures 12 and 13. From these results it is deduced that high values of both SNR and diffraction efficiency are obtained when the reconstruction angle is between  $38^\circ$  and  $41^\circ$  and when  $\delta = 0^\circ$ . When  $\delta = 90^\circ$  noise increases as the signal increases and the level of noise increases when polarization is changed just. That is why the SNR found when  $\delta = 90^\circ$  has lower values than when  $\delta = 0^\circ$  and why it is flatter in shape. We can see this in Figures 14 and 15 in which the response to energy is shown when reconstruction is done in the Bragg angle. Finally, Figures 16 and 17 show the SNR as a function of the reconstruction angle for EDTA and R-10 and when the exposure was  $60 \mu\text{J}/\text{cm}^2$  and the reference-to-object beam ratio was 9.

We analyzed the variation of the SNR and diffraction efficiency as a function of exposure when  $\delta = 0^\circ$  and when the reconstruction angle is  $41^\circ$  because we expected these parameters to have the best values with this angle. Figures 18 and 19 reflect the information we obtained when EDTA and R-10 were used respectively. We must keep in mind that the value of noise was very small for exposures higher than  $120 \mu\text{J}/\text{cm}^2$  in the case of EDTA, at which point noise could not be measured with the photodetector. However, R-10 produced more noise and SNR could be measured up to  $180 \mu\text{J}/\text{cm}^2$ . Therefore, a better SNR can definitely be obtained with EDTA than with R-10.

## 5. CONCLUDING REMARKS

The experimental results shown in this paper indicate that the diffraction efficiency, the signal and the noise of diffuse-object holograms recorded in bleached silver halide emulsion depend largely on the relation between the polarization states of the reference and reconstruction beams. The presence of spurious gratings, generated by

scattering at recording, has been observed in the response of the holograms. It has been experimentally demonstrated that when the polarization of the reconstruction beam is perpendicular to the polarization of the reference beam, the diffraction efficiency of a bleached diffuse-object hologram reconstructed in the Bragg angle is higher than when the two polarizations are parallel only for a specific exposure value which depends on the processing used. Although a change in polarization in the reconstruction step eliminates one source of noise (the noise gratings) the reconstructed image is noisier than the image reconstructed without a polarization change.

Another important result is that when reconstruction is done with the same polarization as used in recording, there are a set of reconstruction angles, larger than the Bragg angle, in which the signal increases but not the noise. This fact produces a simultaneous increase in both the signal-to-noise ratio and the diffraction efficiency.

Finally, the experimental results of this paper give information about possible ways to improve the holographic characteristics of bleached diffuse-object holograms and these results are also important when holograms for optical storage<sup>4,5</sup> or optical interconnections are recorded<sup>3</sup>.

## ACKNOWLEDGMENTS

Part of this work was supported by the *Direcció General d'Ensenyaments Universitaris i Investigació* of the *Generalitat Valenciana*, Spain (Project GV-1165/93).

## REFERENCES

- 1.- R. K. Kostuk, "Comparison of models for multiplexed holograms", **28**, 771-777 (1989).
- 2.- H. Nomura and T. Okoshi, "Storage density limitation of a volume-type hologram memory: Theory", *Appl. Opt.* **15**, 550-555 (1976).
- 3.- R. K. Kostuk, J.W. Goodman and L. Hesselink, "Optical imaging applied to microelectronic chip-to-chip interconnections", *Appl. Opt.* **26**, 3947-3953 (1987).
- 4.- A. Macovski, "Hologram information Capacity", *J. Opt. Am.* **60**, 21-29 (1970).
- 5.- J. R. Wullert II and Yicheng Lu, "Limits of the capacity and density of holographic storage", *Appl. Opt.* **33**, 2192-2196 (1994).
- 6.- H. Kogelnik, "Coupled wave theory for thick hologram gratings", *Bell Syst. Tech. J.* **48**, 290-2947 (1969).
- 7.- A. Beléndez, L. Carretero and A. Fimia, "Experimental evaluation of shearing effects in volume holograms formed in bleached photographic emulsions", *Opt. Laser Tech.* **26**, 341-349 (1994)
- 8.- A. Fimia, L. Carretero, R. Fuentes and A. Beléndez, "Some remarks on noise sources in silver halide volume holograms", *Opt. Eng.* **34**, 1108-1115 (1995).
- 9.- K. Biedermann, "The scattered flux spectrum of photographic materials for holography", *Optik*, **31**, 367-389 (1970).
- 10.- R. R. A. Syms and L. Solymar, "Noise gratings in silver halide volume holograms", *Appl Phys. B* **30**, 177-182 (1983).
- 11.- R. J. Collier *et al.*, "Optical Holography", Academic Press, p. 351 (1971).
- 12.- J. Upatnieks and C. D. Leonard, "Efficiency and image contrast of dielectric holograms", *J. Opt. Soc. Am.* **60**, 297-305 (1970).

- 13.- J. Upatnieks and C. D. Leonard, "Characteristic of dielectric holograms", IBM J. Res. Develop. **14**, 527-532 (1970).
- 14.- A. Fimia, L. Carretero and R. Fuentes, "Volume influence on intermodulation noise of dielectric diffuse-object holograms", Appl. Opt. **31**, 2408-2409 (1992).
- 15.- A. Fimia, A. Beléndez and L. Carretero, "Signal-to-noise ratio of nonlinearly recorded holograms of diffuse objects", Appl. Opt. **33**, 7606-7610 (1994).
- 16.- H. Dammann, "Phase holograms of diffuse-objects", J. Opt. Soc. Am. A **60**, 1635-1639 (1970).
- 17.- H. M. Smith, "Principles of holography", Second Edition, John Wiley & Sons, p. 134 (1975).
- 18.- F. A. Sattarov, "Polarizing properties of thick-film hologram gratings", Opt. Spectrosc. (USSR), **47(4)**, 422-425 (1979).
- 19.- R. K. Kostuk and G. T. Sincerbox, "Polarization sensitivity of noise gratings recorded in silver halide volume holograms", Appl. Opt. **27**, 2993-2998 (1988).
- 20.- A. Beléndez, L. Carretero and I. Pascual, "Polarization influences on the efficiency of noise gratings recorded in silver halide holograms", Appl. Opt. **32**, 7155-7163 (1993).
- 21.- A. Fimia, R. Fuentes and A. Beléndez, "Noise gratings in bleached silver halide diffuse-object holograms", Opt. Lett. **19**, 1243-1245 (1994).
- 22.- R. K. Kostuk, "Factorial optimization of bleach constituents for silver halide holograms", Appl. Opt. **30**, 1611-1616 (1991).
- 23.- A. Beléndez, I. Pascual, R. Fuentes and A. Fimia, "Calculation of shear angles in holographic gratings recorded in bleached silver halide emulsions", Appl. Phys. B **59**, 553-561 (1994).
- 24.- J. R. Fyson, "Bleaching agents and diffusion through gelatin", J. Photogr. Sci. **32**, 234-244 (1984).

## FIGURE CAPTIONS

- Figure 1.- Experimental set up for recording diffuse-object holograms.
- Figure 2.- Diffuse-object geometry.
- Figure 3.- Diffraction efficiency as a function of the reconstruction angle for two values of  $\delta$  when exposure was  $70 \mu\text{J}/\text{cm}^2$ , and EDTA was used.
- Figure 4.- Diffraction efficiency as a function of the reconstruction angle for two values of  $\delta$  when exposure was  $70 \mu\text{J}/\text{cm}^2$ , and R-10 was used.
- Figure 5.- Diffraction efficiency as a function of exposure when the reconstruction angle was the Bragg angle and the bleaching used was EDTA.
- Figure 6.- Diffraction efficiency as a function of exposure when the reconstruction angle was the Bragg angle and the bleaching used was R-10.
- Figure 7.- Noise as a function of the reconstruction angle for two values of  $\delta$  when the level of exposure was  $70 \mu\text{J}/\text{cm}^2$  and the bleaching used was EDTA.
- Figure 8.- Noise as a function of the reconstruction angle for two values of  $\delta$  when the level of exposure was  $70 \mu\text{J}/\text{cm}^2$  and the bleaching used was R-10.
- Figure 9.- Noise as a function of the reconstruction angle when the processing has a fixation step.
- Figure 10.- Signal and noise as a function of the reconstruction angle when the level of exposure was  $70 \mu\text{J}/\text{cm}^2$  and  $\delta = 0^\circ$ . The processing used was EDTA.
- Figure 11.- Signal and noise as a function of the reconstruction angle when the level of exposure was  $70 \mu\text{J}/\text{cm}^2$  and  $\delta = 0^\circ$ . The processing used was R-10.
- Figure 12.- Signal and noise as a function of the reconstruction angle when the level of exposure was  $70 \mu\text{J}/\text{cm}^2$  and  $\delta = 90^\circ$ . The processing used was EDTA.

Figure 13.- Signal and noise as a function of the reconstruction angle when the level of exposure was  $70 \mu\text{J}/\text{cm}^2$  and  $\delta = 90^\circ$ . The processing used was R-10.

Figure 14.- SNR as a function of exposure when the reconstruction angle was the Bragg angle. The beam ratio was  $K = 9$  and the processing used was EDTA.

Figure 15.- SNR as a function of exposure when the reconstruction angle was the Bragg angle. The beam ratio was  $K = 9$  and the processing used was R-10.

Figure 16.- SNR as a function of the reconstruction angle two values of  $\delta$  when exposure was  $60 \mu\text{J}/\text{cm}^2$ . The processing used was EDTA and the beam ratio was  $K = 9$ .

Figure 17.- SNR as a function of the reconstruction angle two values of  $\delta$  when exposure was  $60 \mu\text{J}/\text{cm}^2$ . The processing used was R-10 and the beam ratio was  $K = 9$ .

Figure 18.- Diffraction efficiency and signal-to-noise ratio as a function of exposure when the reconstruction angle was  $37.5^\circ$  and when  $\delta = 0^\circ$ . The processing used was EDTA.

Figure 19.- Diffraction efficiency and signal-to-noise ratio as a function of exposure when the reconstruction angle was  $37.5^\circ$  and when  $\delta = 0^\circ$ . The processing used was R-10.

## TABLES

Table I.- Processing schedule.

Table II.- Developer and bleach bath formulas.



**TABLE I**

<b>Step Procedure</b>	<b>Time (min)</b>
1. Develop	3
2. Rinse in running water	1
3. Bleached	≈ 3
4. Wash in running water	5

*All solutions at 20 °C*

TABLE II

---

<b><i>PAAAC developer</i></b>	
Sodium carbonate	120 g
Ascorbic acid	18 g
Phenidon	0.5 g
Distilled water	1 litre
<b><i>R-10 Rehalogenating bleach bath</i></b>	
Potassium dichromate	2 g
Shulphuric acid	10 ml
Potassium bromide	35 g
Distilled water to make	1 litre
<b><i>EDTA Rehalogenating bleach bath</i></b>	
Ferric sulfate	30 g
Potassium bromide	30 g
Shulphuric acid	10 ml
Distilled water to make	1 litre

---

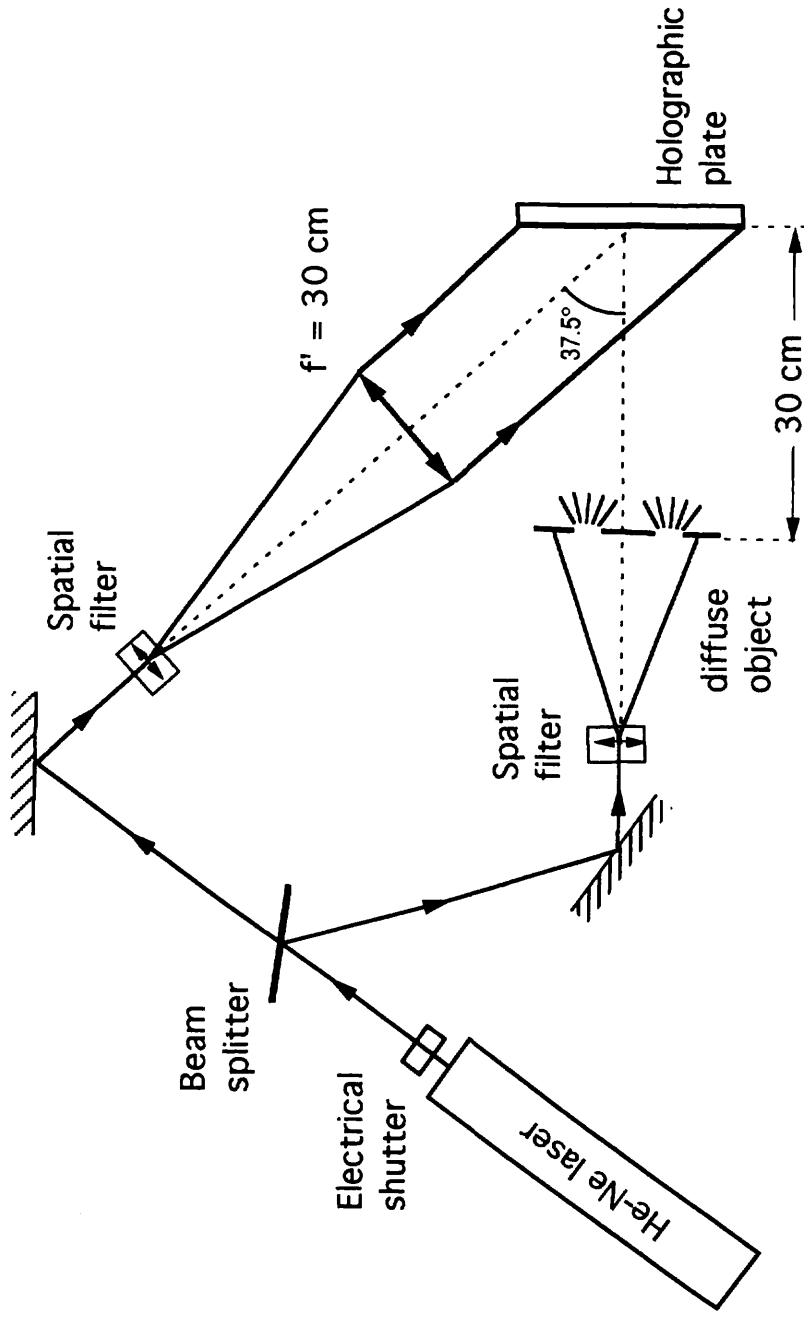


FIGURE 1  
A.Fimia et al.

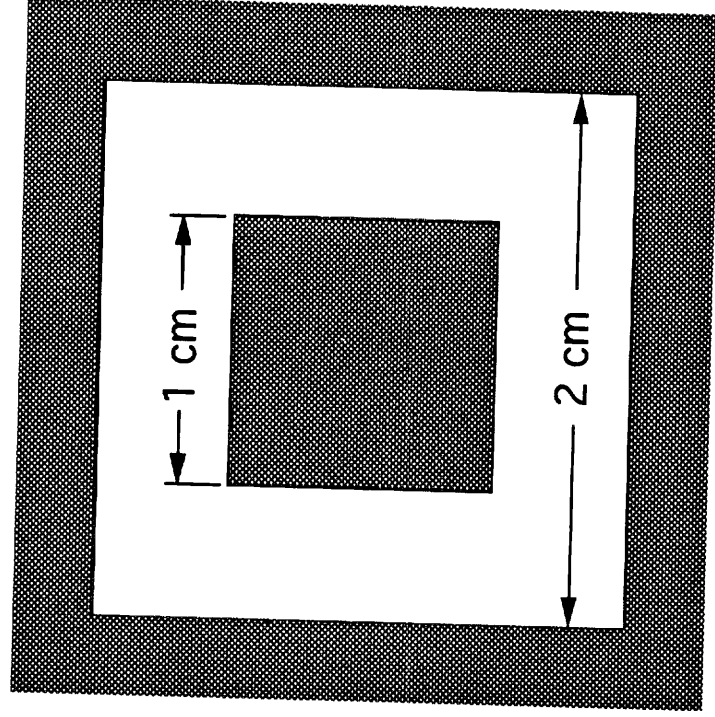


FIGURE 2  
A.Fimia et al.

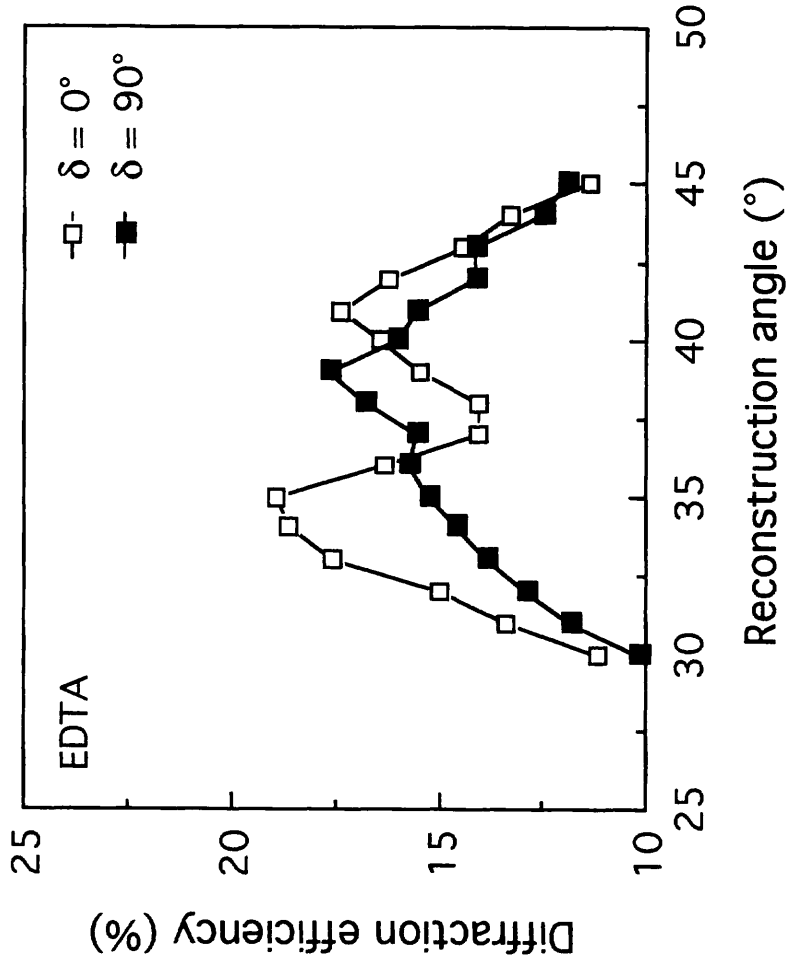


FIGURE 3  
A, Finia et al.

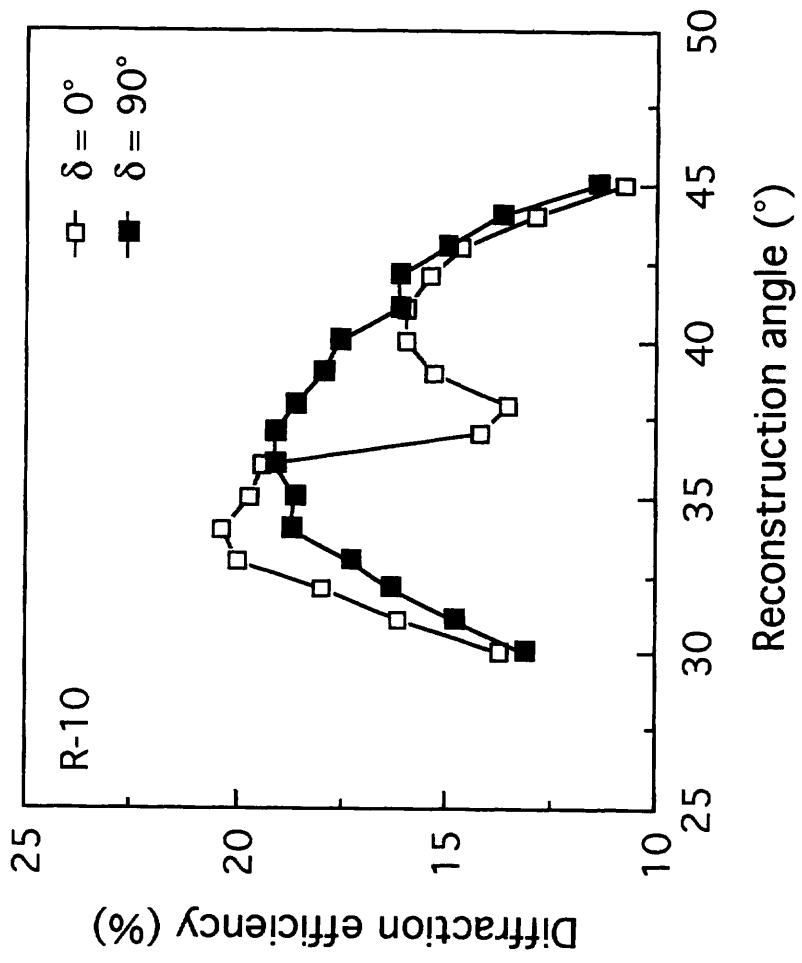


FIGURE 4  
A. Fimia et al.

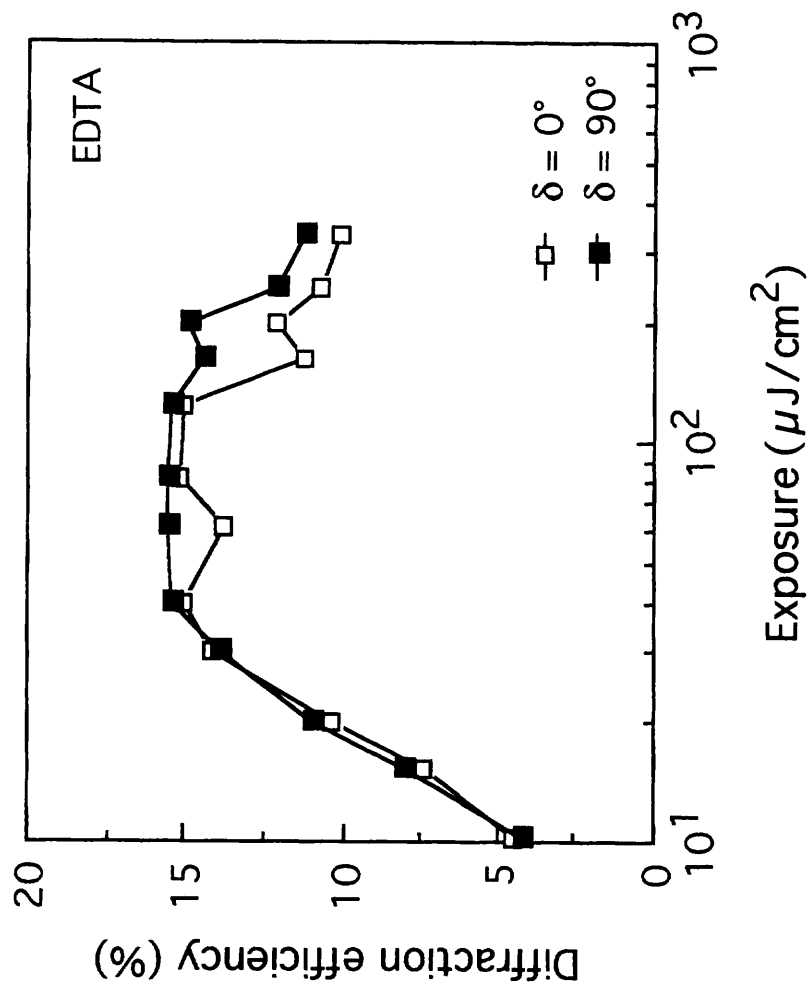


FIGURE 5  
A. Fimia et al

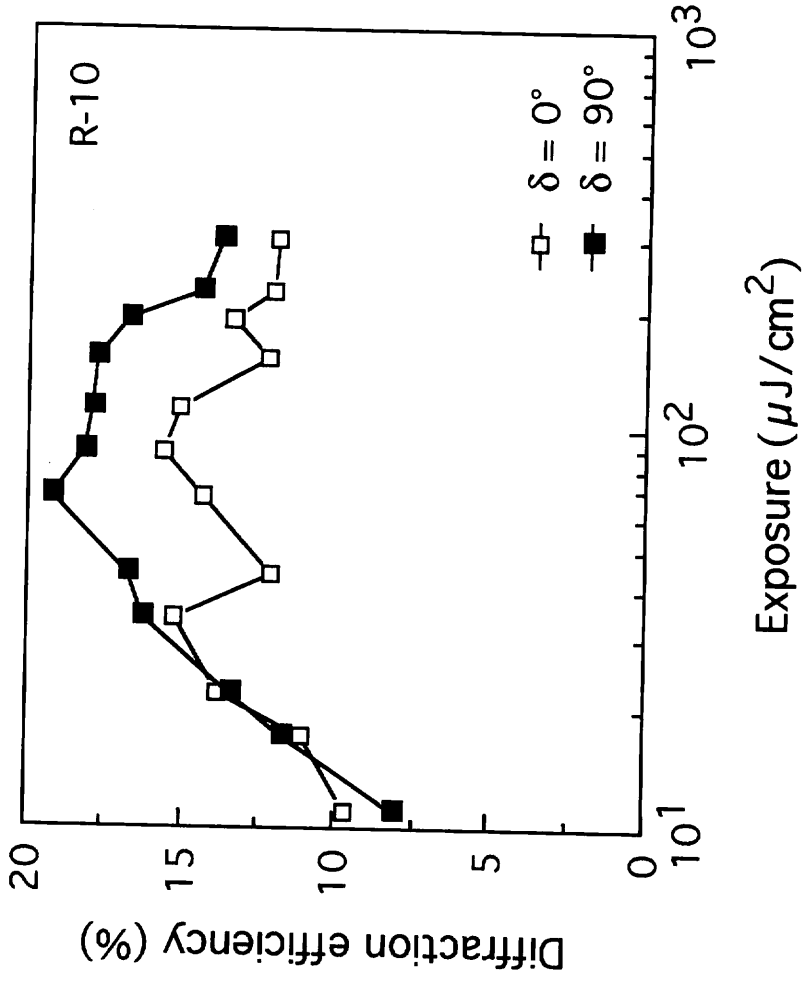


FIGURE 6  
A. Fimia et al.



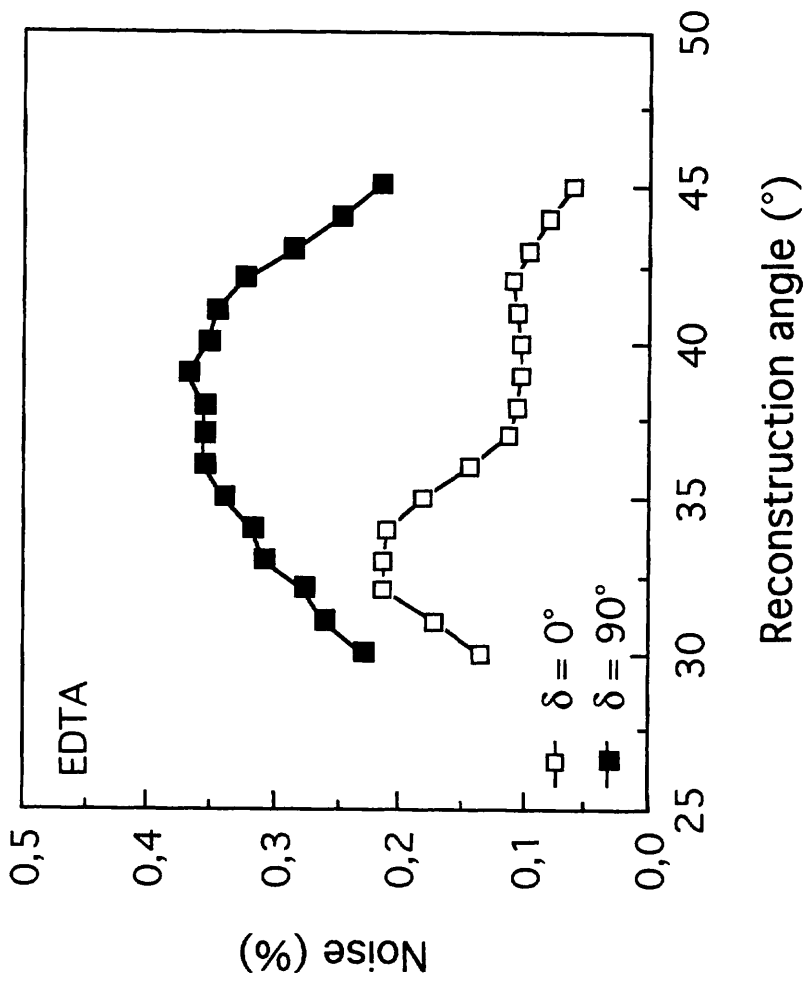


FIGURE 7  
A. Fimia et al.

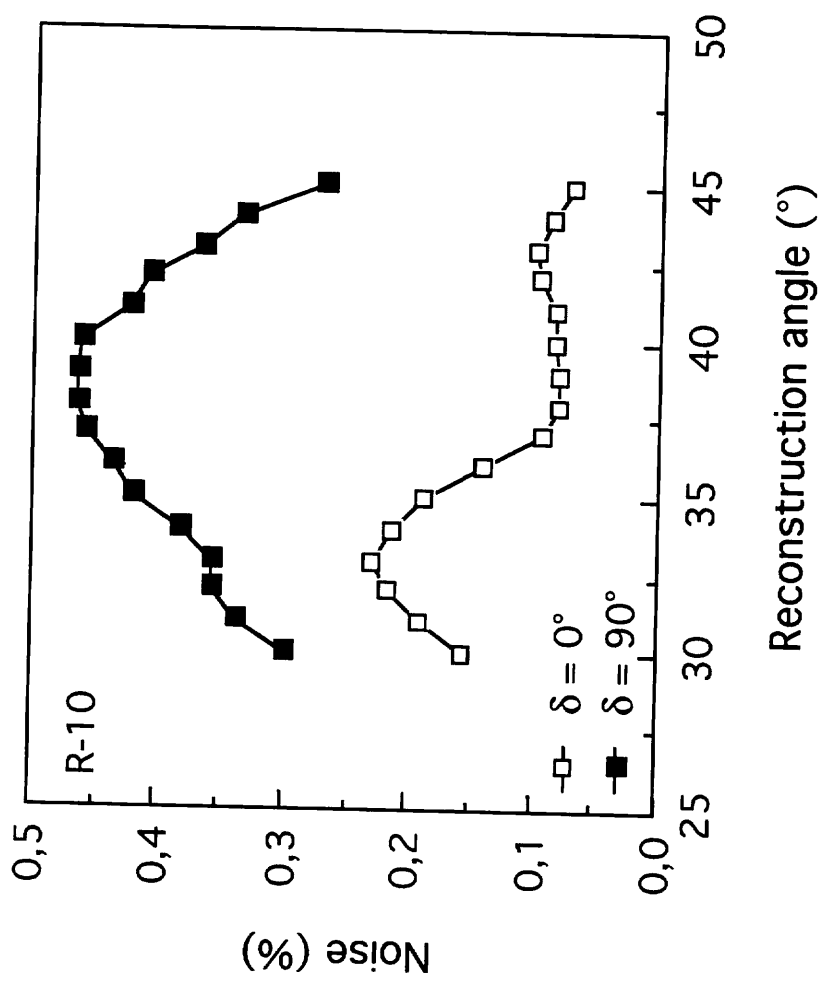


FIGURE 8  
A.Fimia et al.

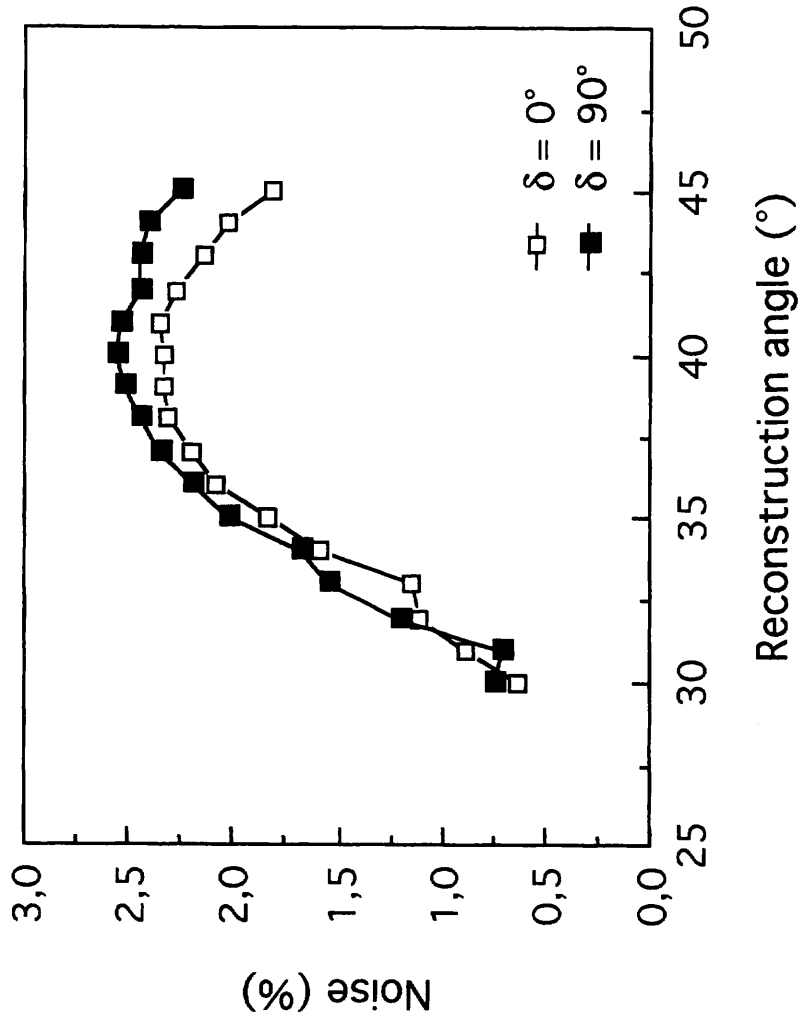


FIGURE 9  
A.Fimia et al.

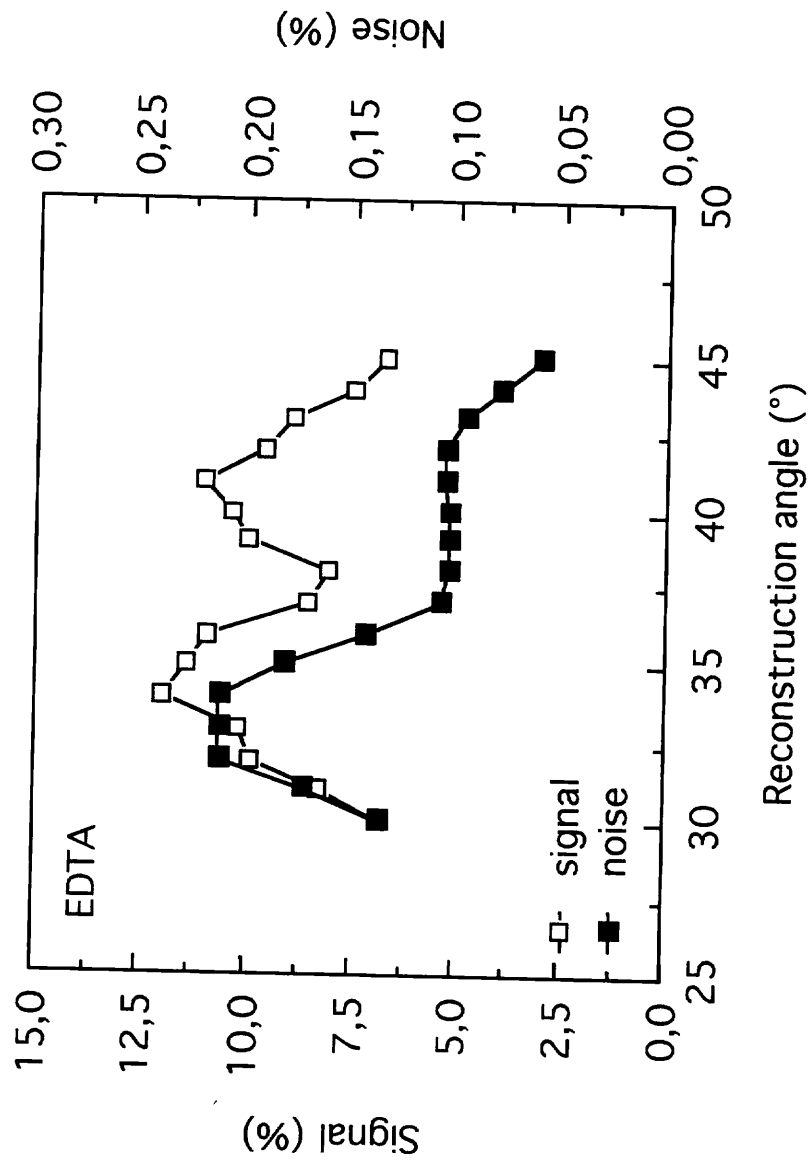


FIGURE 10  
A.Fimia et al.

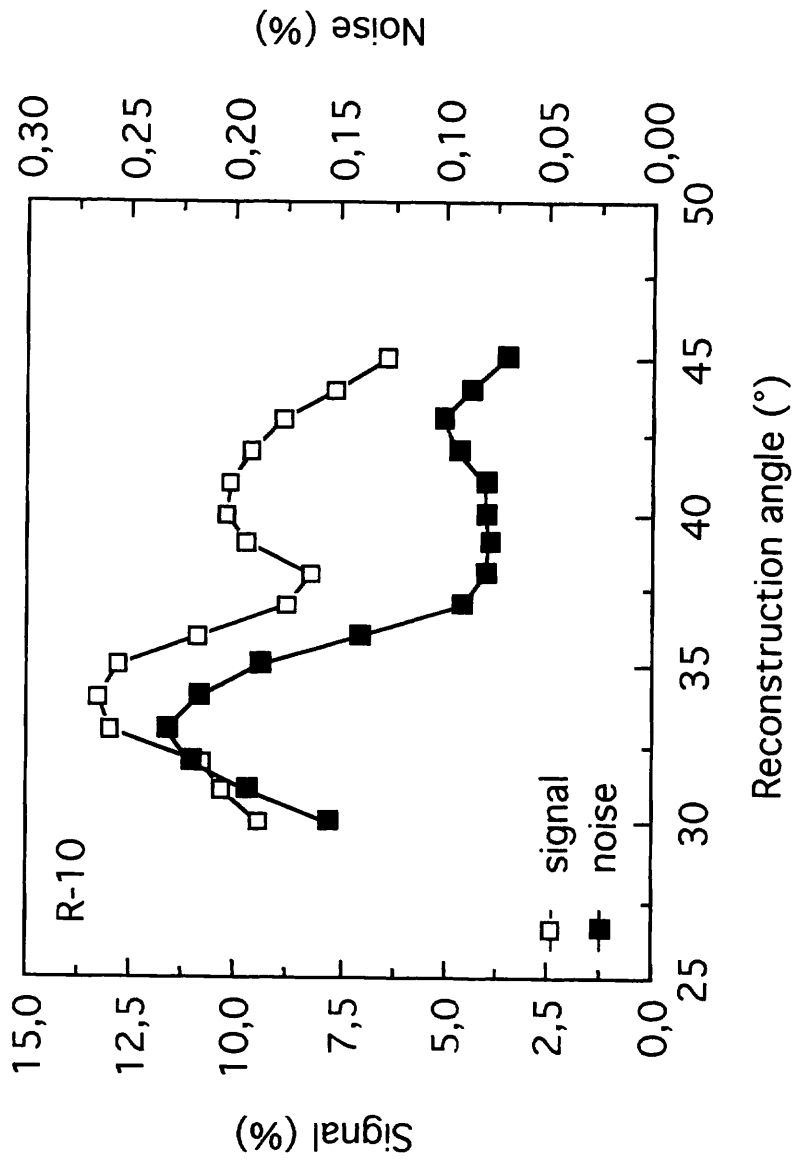


FIGURE 11  
A. Fimia et al.

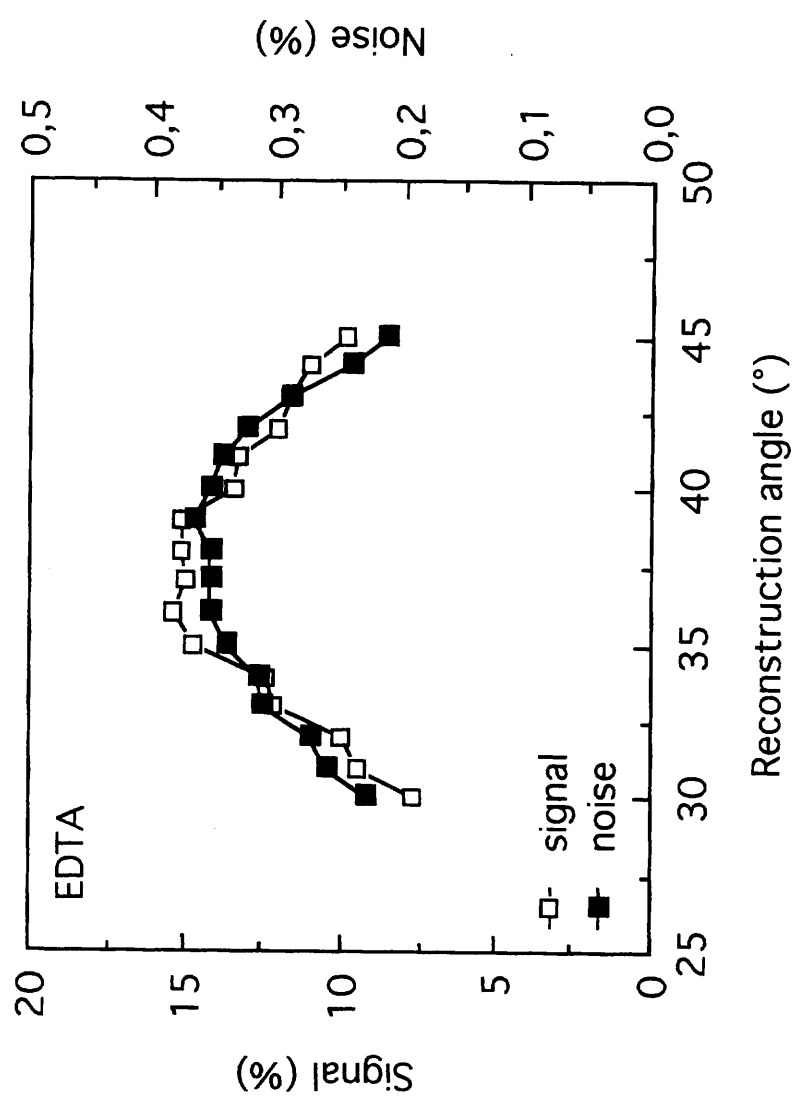


FIGURE 12  
A.Fimia et al.

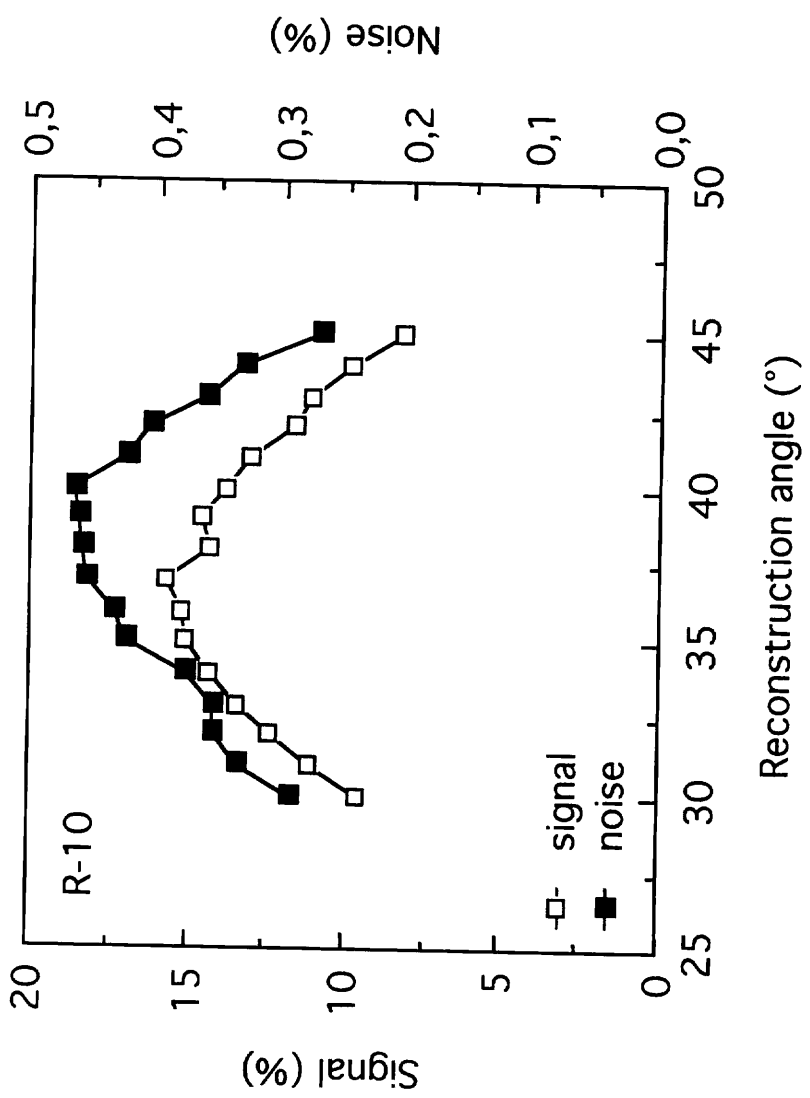


FIGURE 13  
A.Fimia et al.

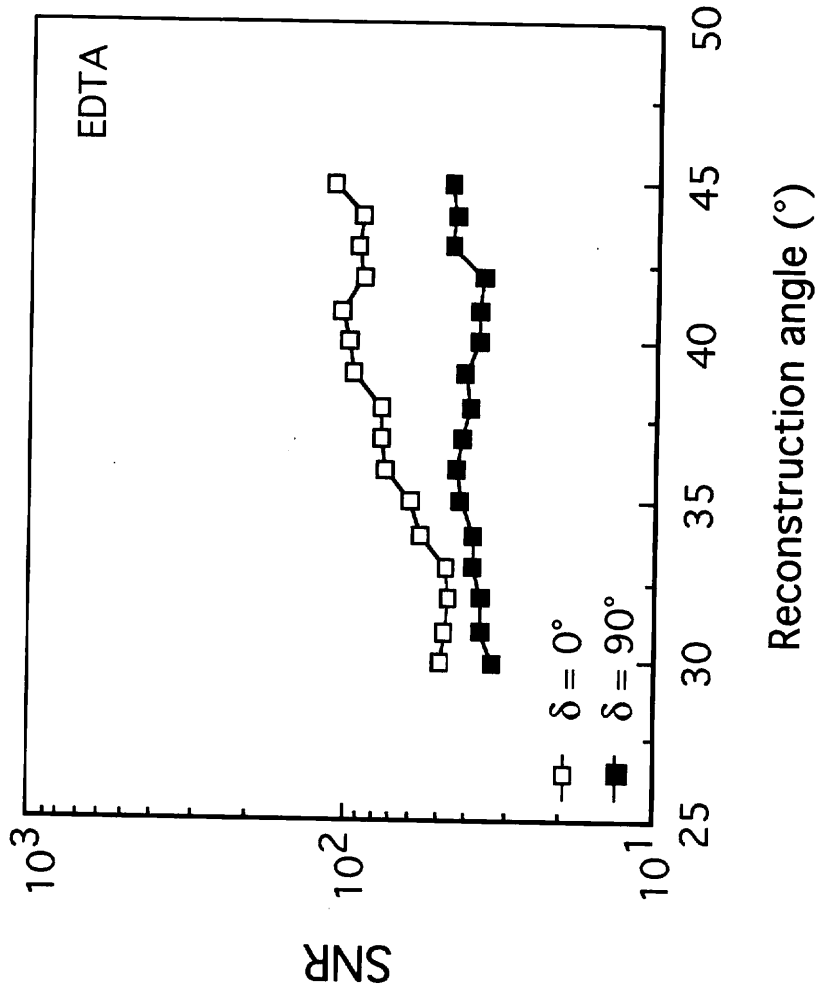


FIGURE 14  
A.Fimia et al.



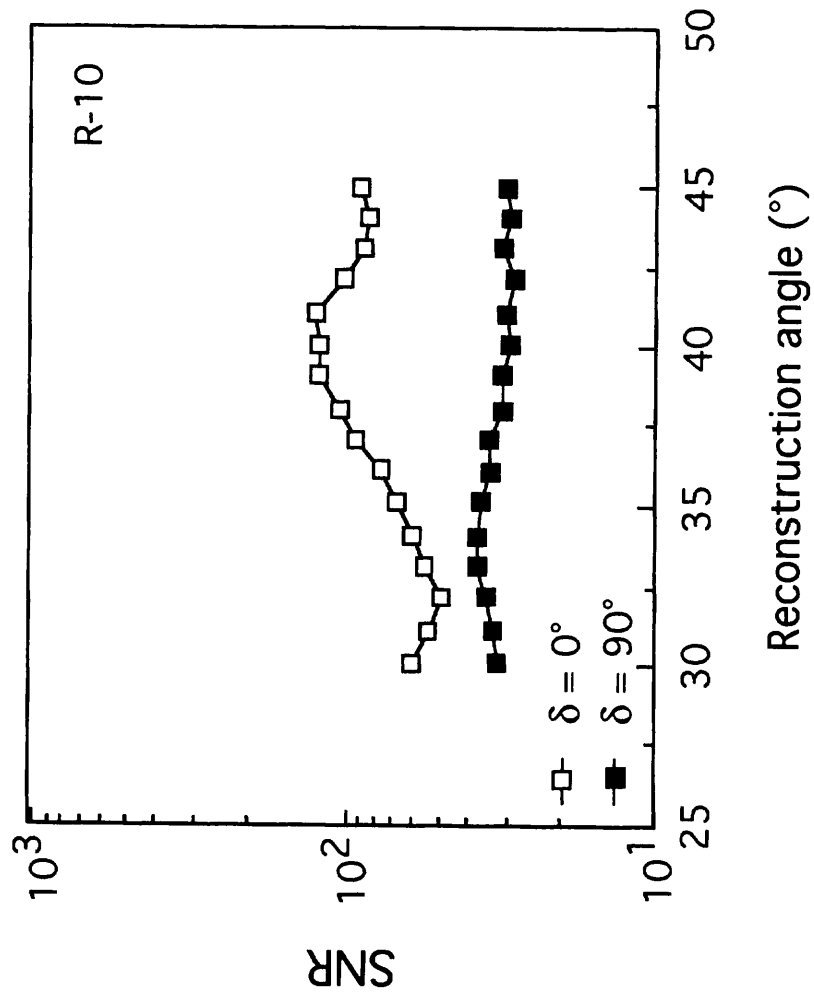


FIGURE 15  
A. Fimia et al.

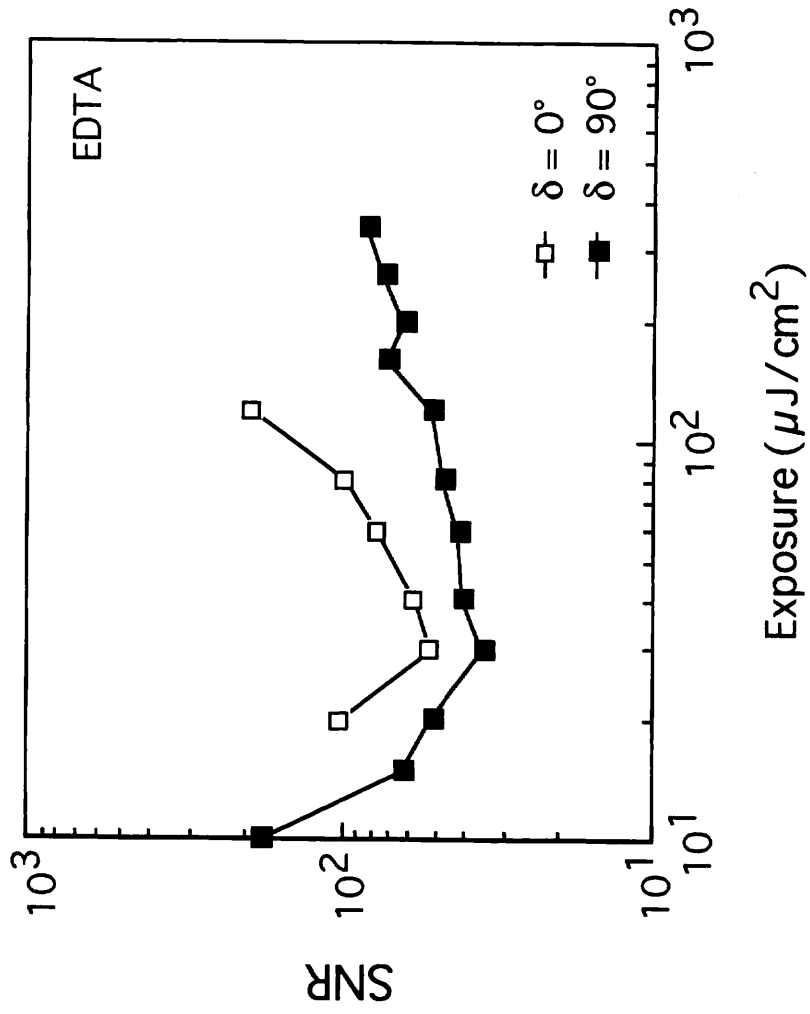


FIGURE 16  
A. Fimia et al.

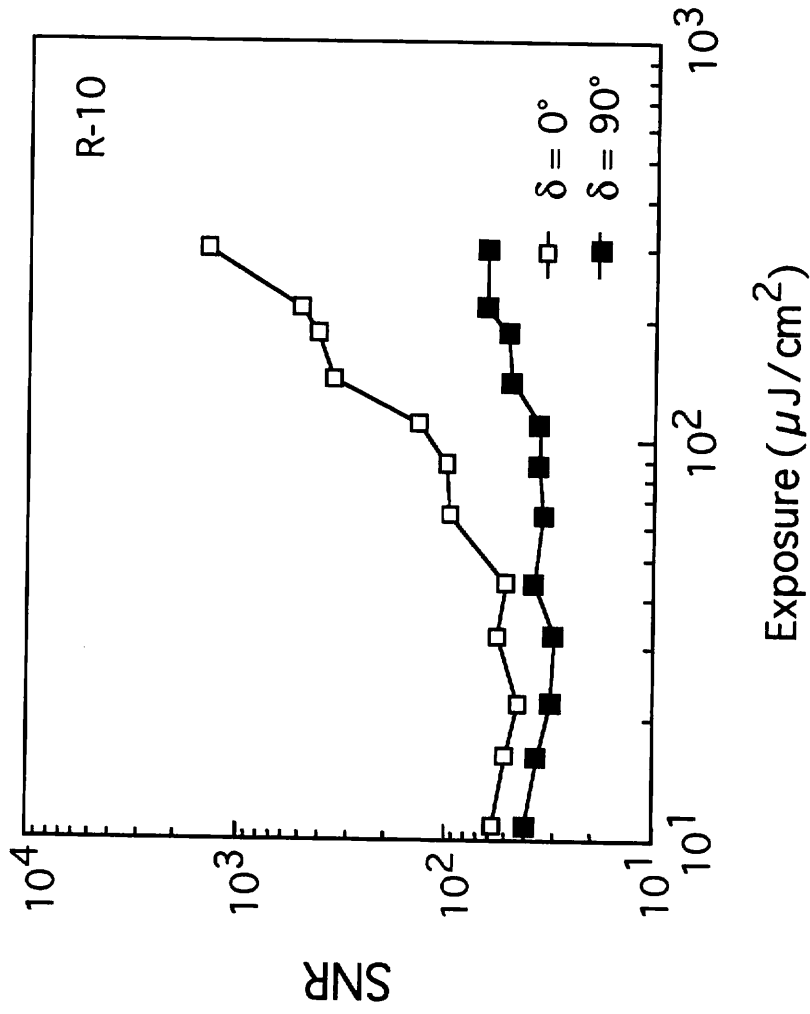


FIGURE 17  
A. Fimia et al.

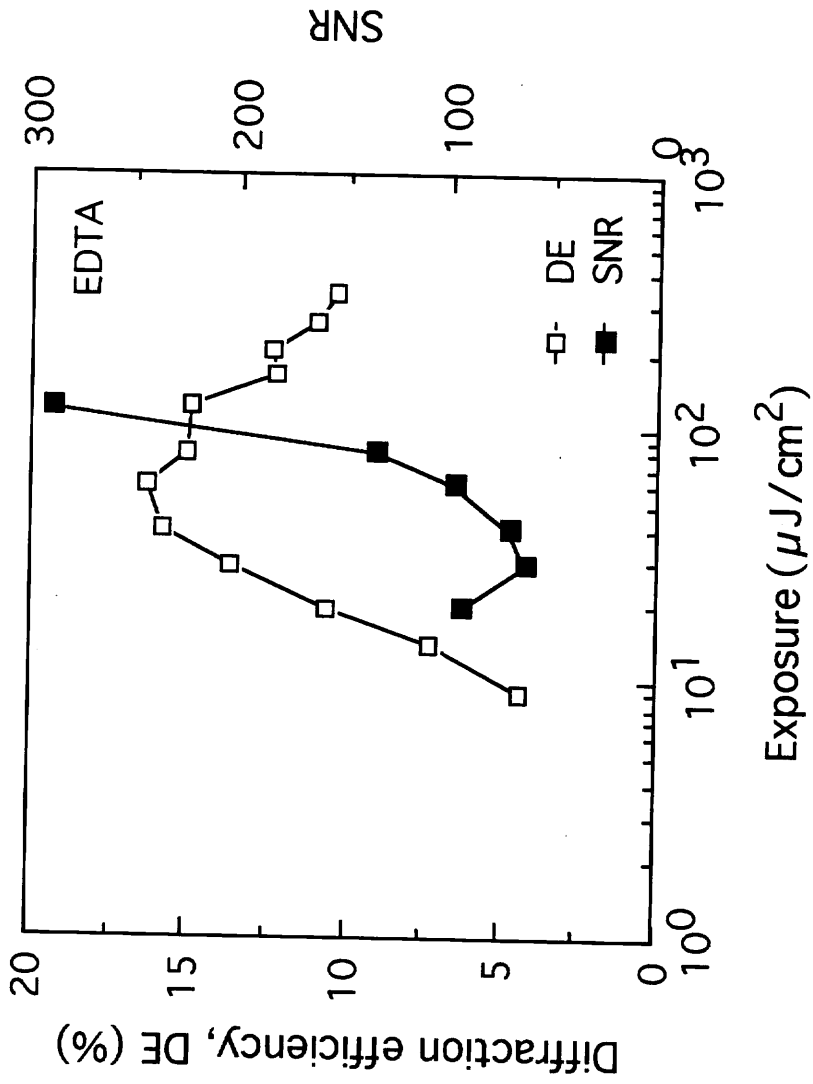


FIGURE 18  
A. Fimia et al.

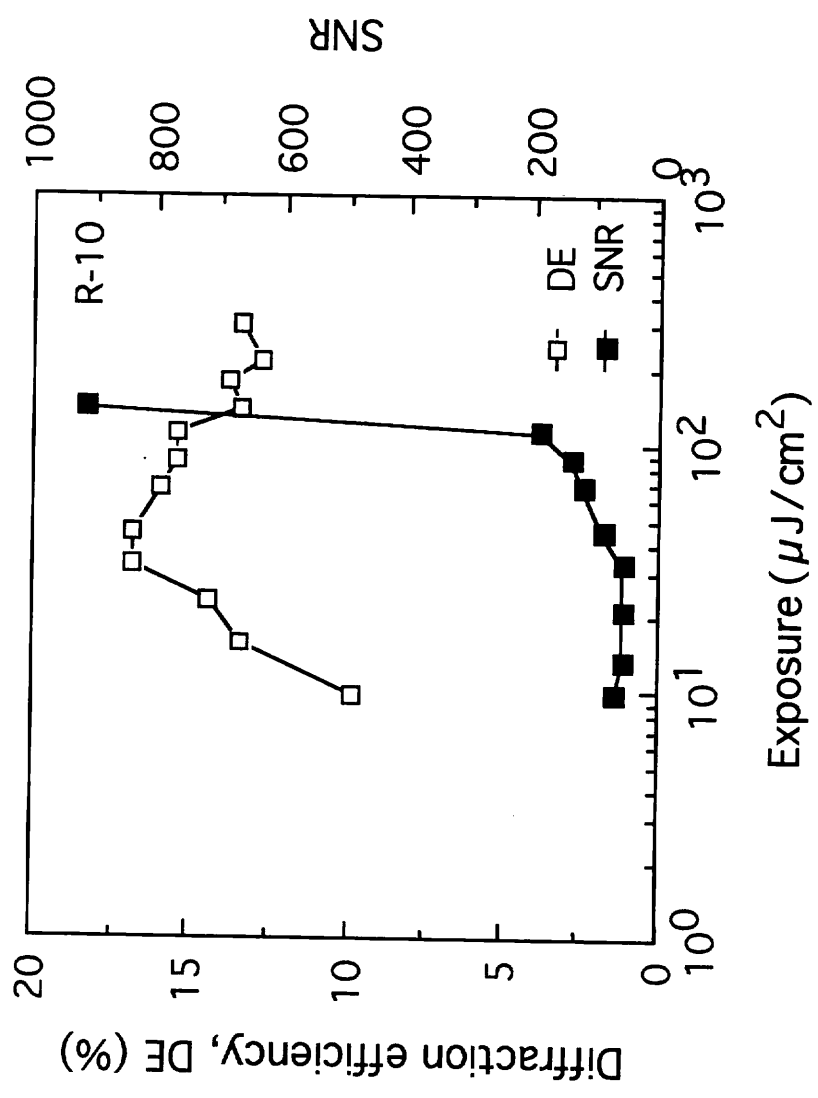


FIGURE 19  
A.Fimia et al.